

Supplementary Information

Mixed Ligand Copper(II)-Diimine Complexes of 2-Formylpyridine-*N*⁴-Phenylthiosemicarbazone: Diimine Co-ligands Tune the in Vitro Nanomolar Cytotoxicity

Radhakrishnan Kartikeyan,^a Dhanashree Murugan,^b Tamilarasan Ajaykamal,^c Manikandan Varadhan,^a Loganathan Rangasamy,^b Marappan Velusamy,^d Mallayan Palaniandavar^{c*} and Venugopal Rajendiran^{*a}

^a*Department of Chemistry, School of Basic and Applied Sciences, Central University of Tamil Nadu, Thiruvarur 610005, India*

^b*Drug Discovery Unit (DDU), Centre for Biomaterials, Cellular and Molecular Theranostics (CBCMT), Vellore Institute of Technology (VIT), Vellore 632014, Tamil Nadu, India*

^c*Department of Chemistry, Bharathidasan University, Tiruchirappalli 620024, India*

^d*Department of Chemistry, North Eastern Hill University, Shillong 793022, India*

DNA binding studies

EthBr displacement assay

The competitive binding studies of [CuL]⁺ and **1-6** with EthBr were conducted by fluorescence emission spectroscopy to observe if the complexes could displace EthBr from the DNA-EthBr conjugate. The DNA-EthBr conjugate was prepared by pre-treating 12.5 μM EthBr and 125 μM CT-DNA (1:10 ratio) for 5 min in Tris-HCl buffer solution. The emission intensity of EthBr was used as a spectral probe, which was meant to enhance emission intensity due to the intercalative binding mode of EthBr to CT-DNA. EthBr showed reduced emission intensity in buffer solution because of solvent quenching. Hence, emission intensity decreases based on the ability of metal complexes to replace EthBr-DNA conjugate. The apparent DNA binding constants (*K*_{app}) were determined from the extent of reduction of the EthBr emission intensity using the equation.

$$K_{EthBr}[EthBr] = K_{app}[complex] \dots\dots\dots (2)$$

Where *K*_{EthBr} is 1 x 10⁷ M⁻¹,¹, the concentration of EthBr is 12.5 μM, and the concentration of the complex is that used to obtain a 50% reduction of fluorescence intensity of EthBr.

Viscosity experiments

To determine the nature of molecular interaction of the complexes with the CT-DNA, the change in viscosity of DNA was measured by a Ubbelohde viscometer by maintaining a constant temperature at 20 °C.² U The complex was added gradually in increasing concentration from 1/R 0 to 0.5 to 100 mM of DNA stock solution present in 10% DMF-Tris-

HCl buffer, and the viscosity was measured for each addition. The mixture was equilibrated for 5 min before each addition. The data thus obtained were plotted as $(\eta/\eta_0)^{1/3}$ versus $1/R$, where η and η_0 are the viscosity of DNA in the presence of the complex and the viscosity of DNA alone in buffer solution, respectively.^{3,4}

DNA cleavage studies

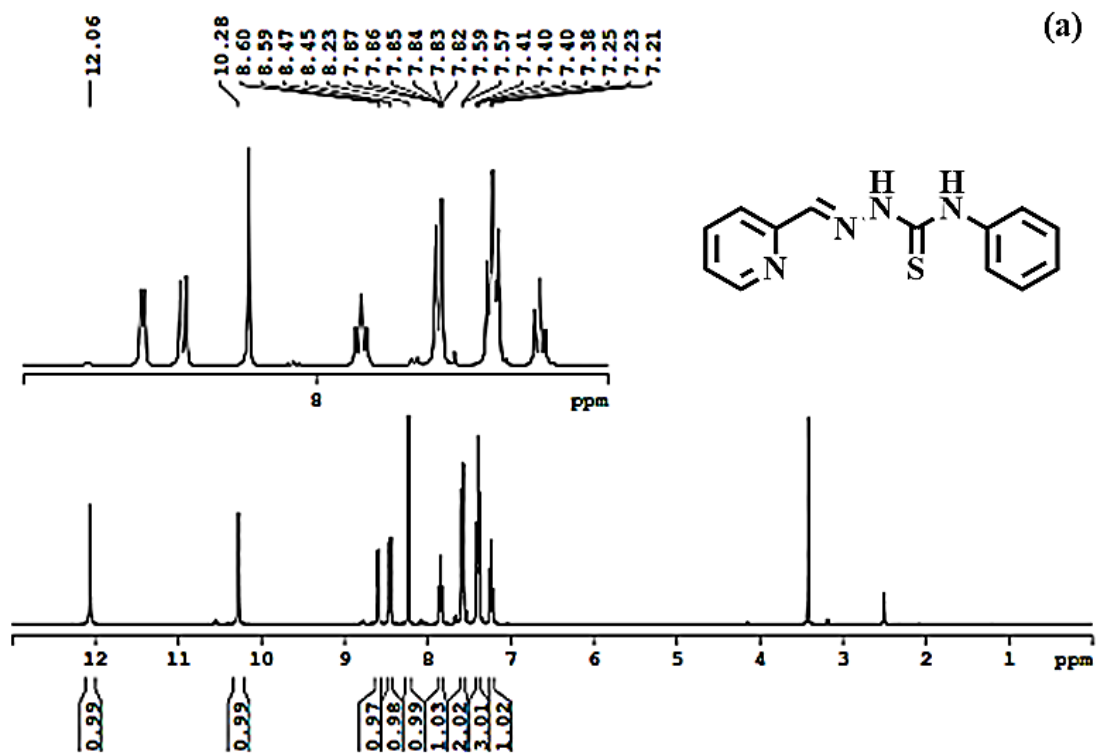
The DNA cleavage activity of copper complexes was investigated by agarose gel electrophoresis. In a typical experiment, plasmid DNA (40 μ M) was mixed with copper(II) complexes $[\text{CuL}]^+$ and **1-6** (100 μ M) for self-activating cleavage reaction and 50 and 100 μ M for oxidative cleavage reaction. For oxidative cleavage, ascorbic acid was used as a reducing agent (25 and 50 μ M). The following experiments were carried out in Tris-HCl buffer to minimize the DMF concentration of copper complexes dissolved in DMF solvent. Supercoiled plasmid DNA was treated with Cu(II) complexes in a clean Eppendorf tube without and with the activating agent and was incubated at 37 °C for 4 h and 1 h, respectively. At the end of incubation, the reaction was quenched by adding loading buffer (7 mM EDTA, 0.15% bromophenol blue, 0.15% xylene cyanol, and 75% glycerol) and loaded with 1% agarose gel containing 1mg/mL EthBr.⁵ The gel was run at 50 V for 3-5 h in TAE buffer (pH 8.0; 40 mM tris base, 20 mM acetic acid, 1 mM EDTA). The gels were documented using a Gel documentation system, and images were captured using a CCD camera (Alpha InfoTech Corporation). Densitometric calculations were made using ImageJ software. A correction factor of 1.47 was used for supercoiled DNA (Form I) assessment because of the weak intercalation of EthBr to supercoiled (Form I) compared to nicked (Form II) and linear DNA (Form III).⁶

The experiment was carried out in the presence of various radical scavengers to elucidate the DNA cleavage mechanism. In these experiments, DMSO (0.1 M), NaN_3 (100 μ M), Catalase (6 units), and Superoxide dismutase (4 units) were added alternatively to the solution containing supercoiled DNA and active copper complex. In addition to that anaerobic experiment was performed by purging the DNA-complex mixture with N_2 . The mixture was incubated to initiate the reaction, then the subsequent treatment and analysis followed the described procedures above.

Protein binding study or tryptophan fluorescence quenching

Quenching of the tryptophan residues of BSA or HSA was done using complexes as quenchers. Steady-state emission studies of the complexes were carried out by the addition of

the various concentrations of complexes (0-60 μM) while keeping the concentration of HSA constant. Concentrated stock solutions of metal complexes were prepared by dissolving them in 10% DMF/ $\text{NaH}_2\text{PO}_4\text{:NaHPO}_4$ buffer at pH 6.8 or 7.1 of metal complexes and diluting further with suitable buffer to attain the required concentration for all the experiments. Upon incremental addition of quencher to the solutions of HSA, the emission intensity was recorded (excitation wavelength at 295 nm)^{1,7} in ranges 300-500 nm. All measurements were made at 25 $^\circ\text{C}$ in a thermostated cuvette holder with a 5 nm slit in each in and out pathway. To determine the interaction of metal complexes with albumin proteins, Stern-Volmer equations⁸ and The I/I_0 versus [complex] graphs were used to obtain the dynamic quenching constant K_{SV} (in M^{-1}).



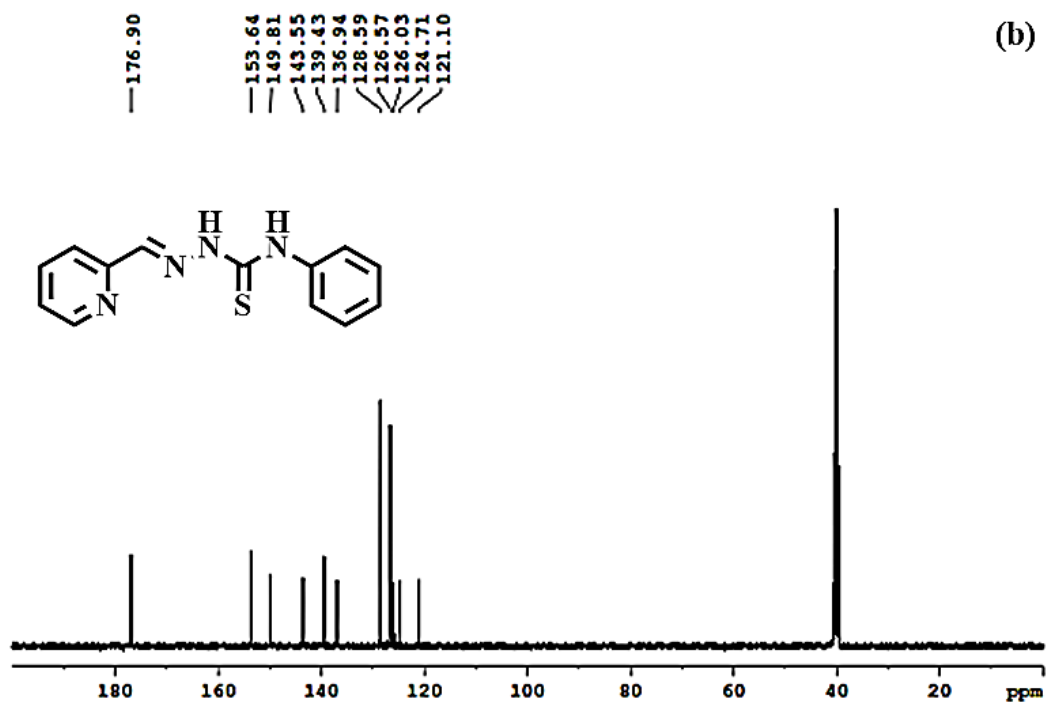
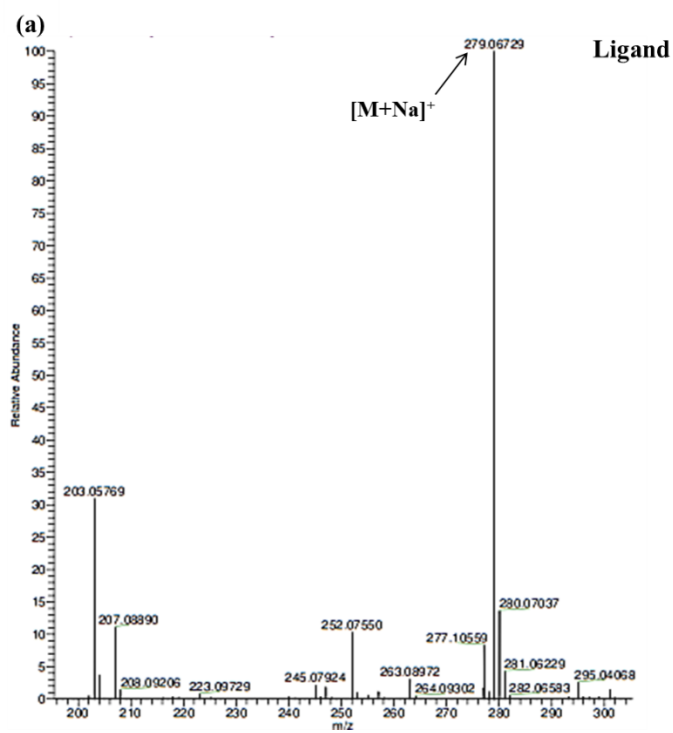
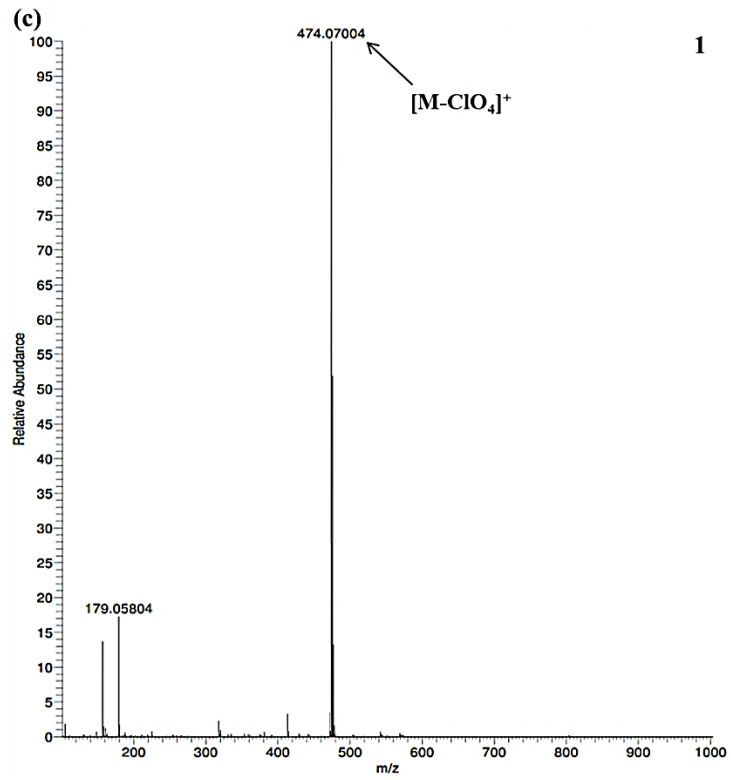
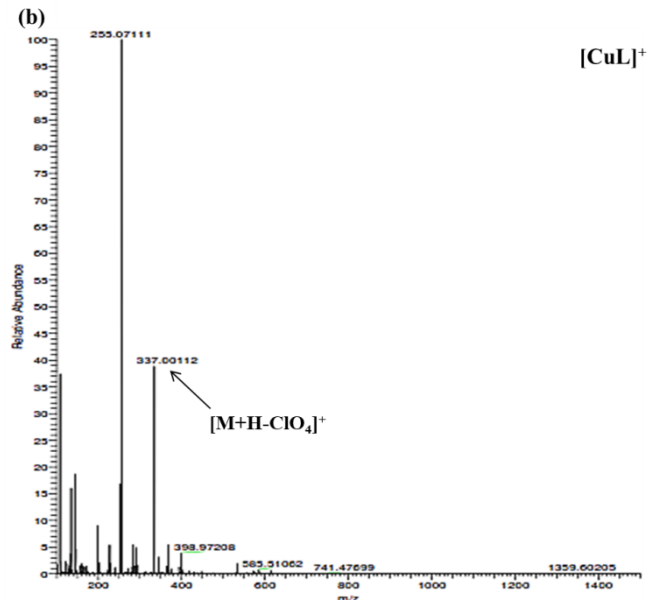
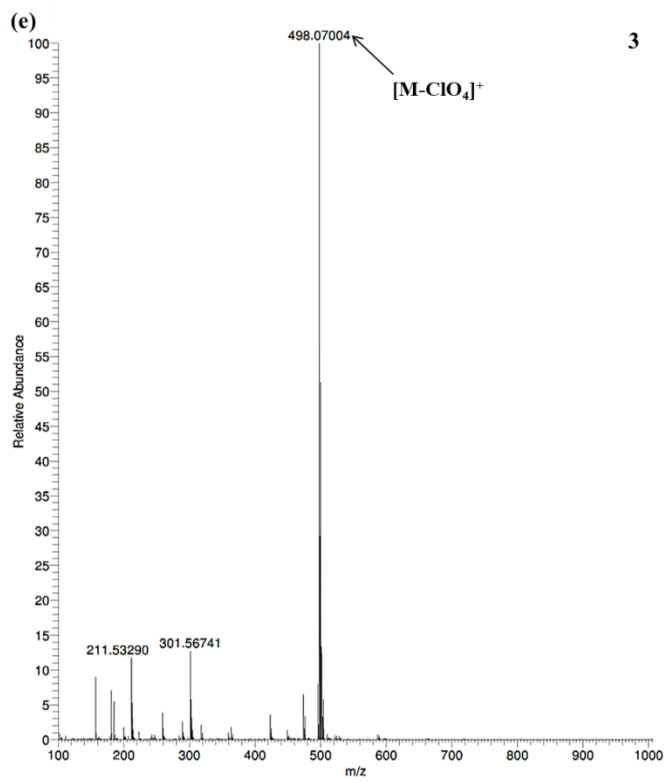
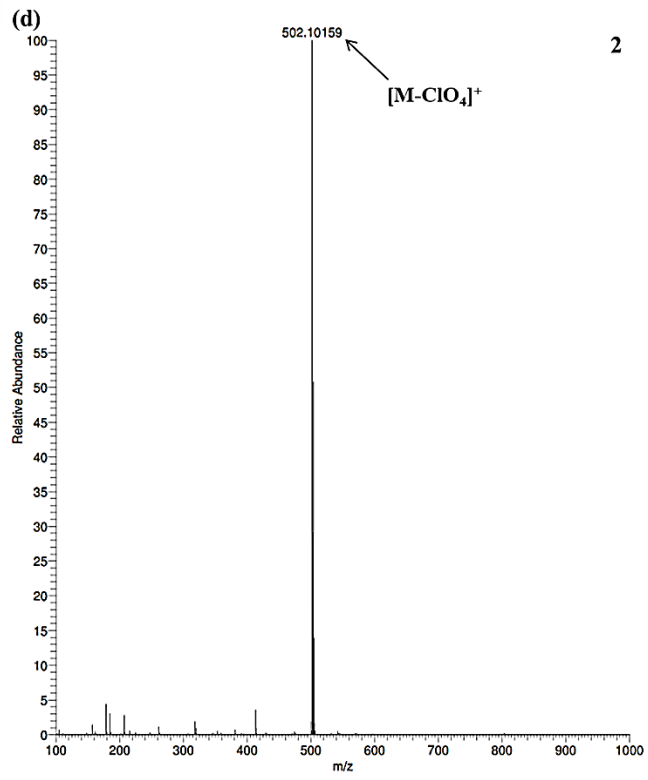
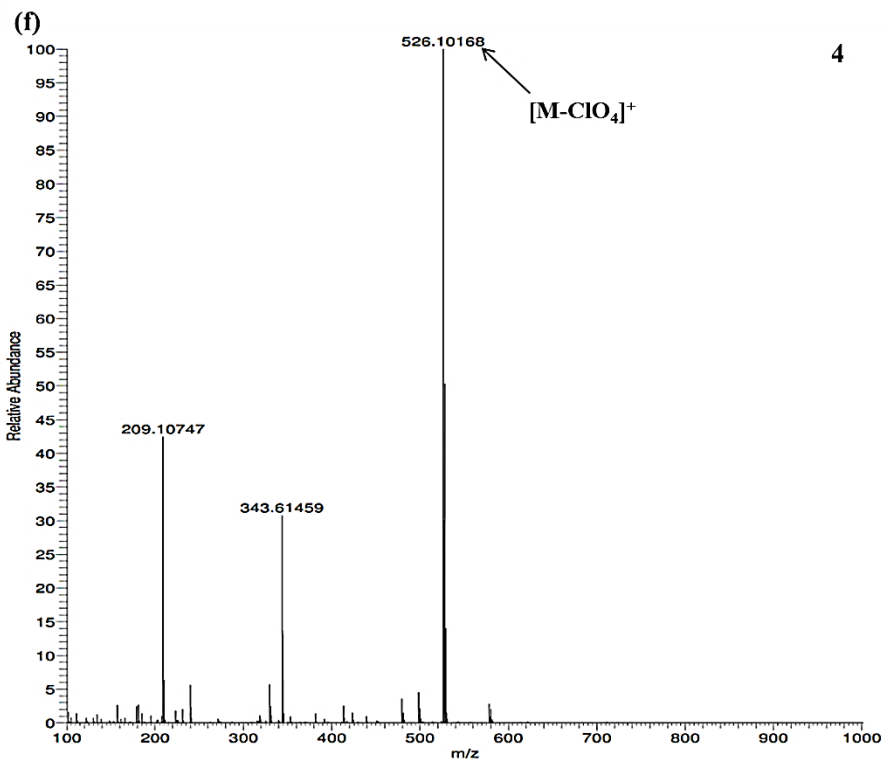


Figure S1. (a) ^1H -NMR and (b) ^{13}C -NMR spectra of ligand in DMSO-d_6 .

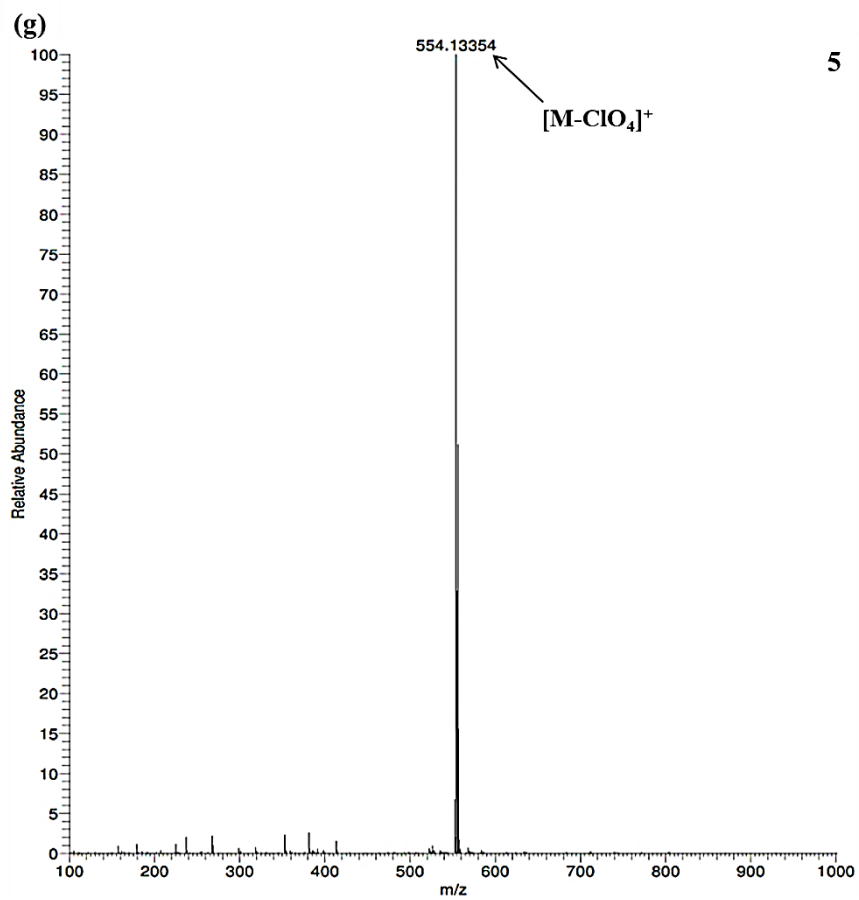








4



5

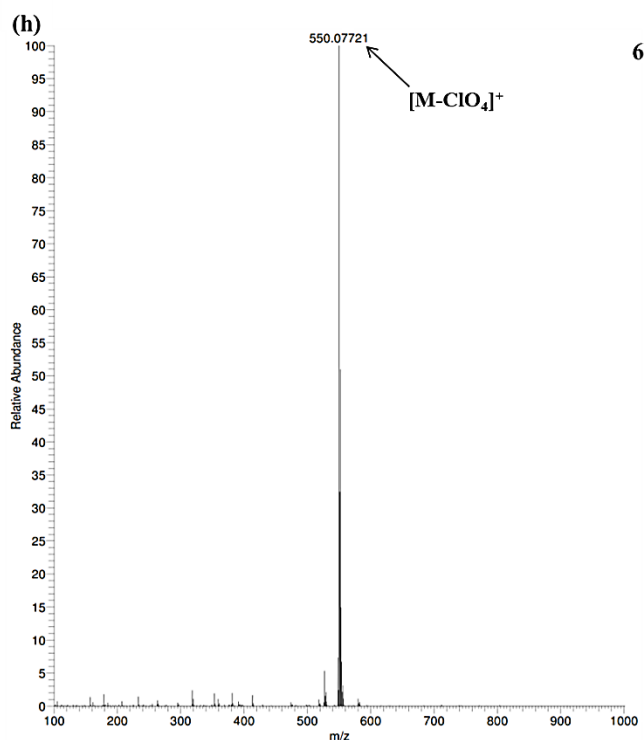


Figure S2. (a)-(h) HRMS spectrum of ligand and copper(II) complexes [CuL]⁺ and 1-6 in methanol.

Table S1. Molar conductance values for copper(II) complexes [CuL]⁺ and 1-6 in DMF

S. No.	Complex	$\Lambda_m(\text{Scm}^2\text{mol}^{-1})$
1	[CuL] ⁺	64
2	1	83
3	2	69
4	3	66
5	4	51
6	5	47
7	6	72

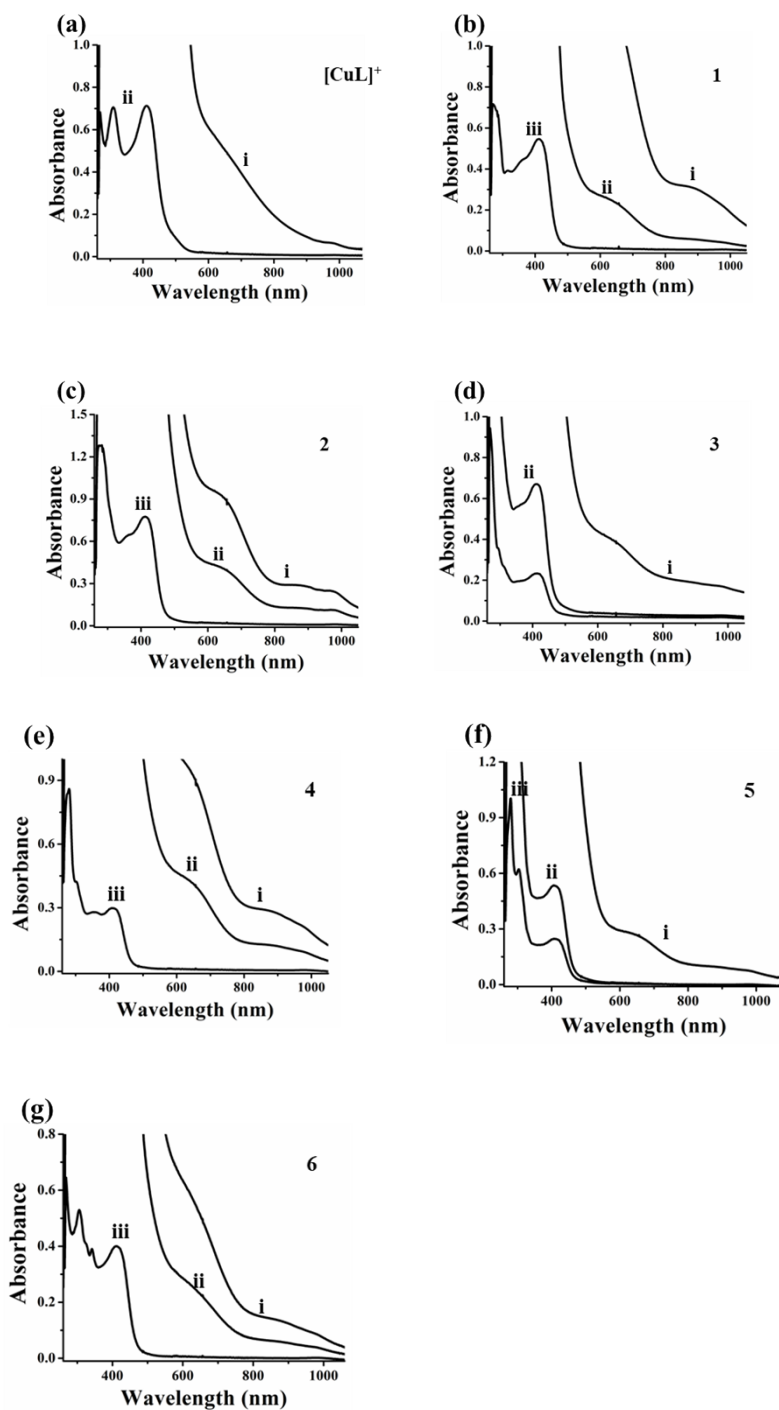
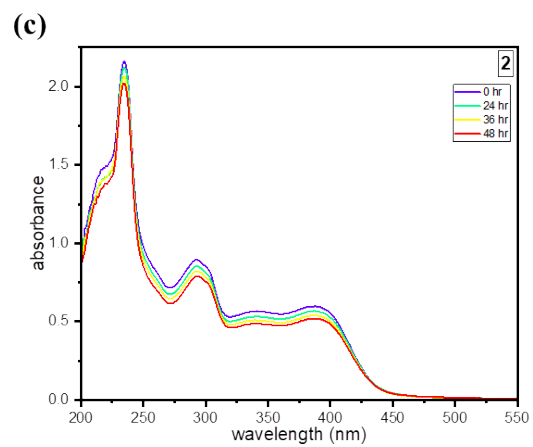
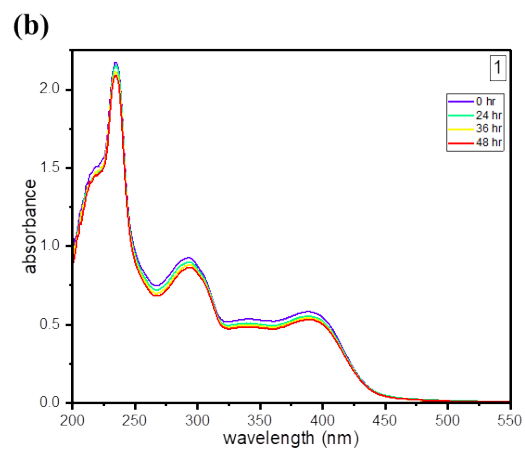
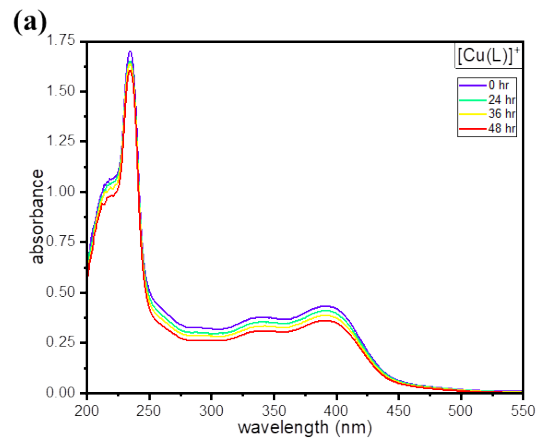
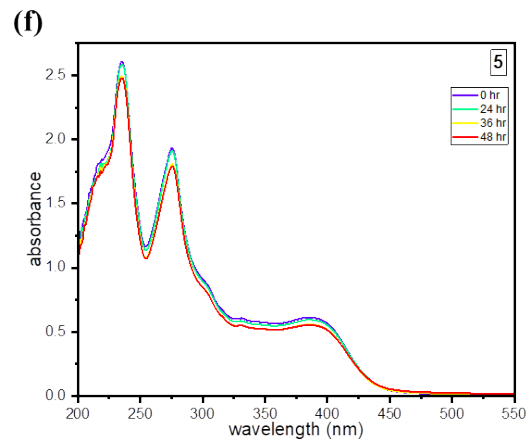
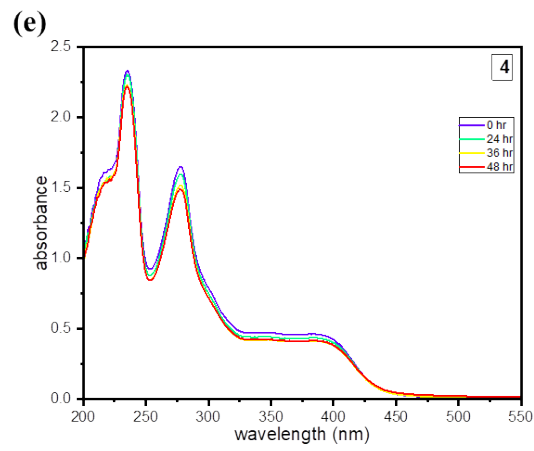
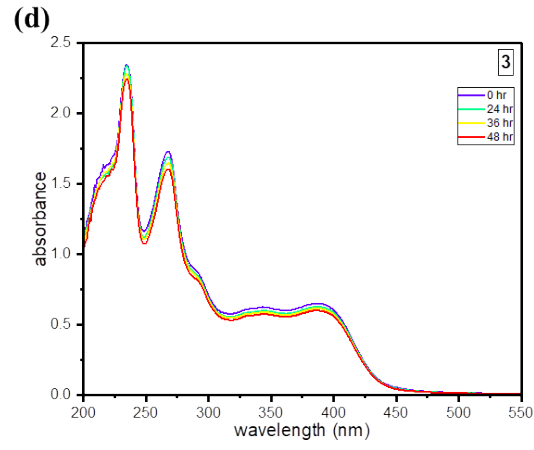


Figure S3. (a)-(g) Electronic absorption spectra of complexes $[\text{CuL}]^+$ and **1-6** in 10% DMF-Tris-HCl buffer (Concentration (i-iv): 5×10^{-3} to 1×10^{-5} M).





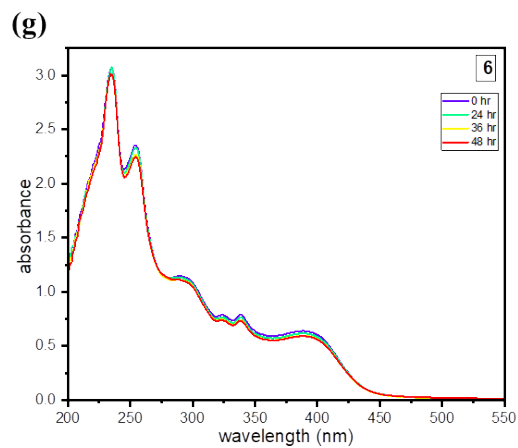
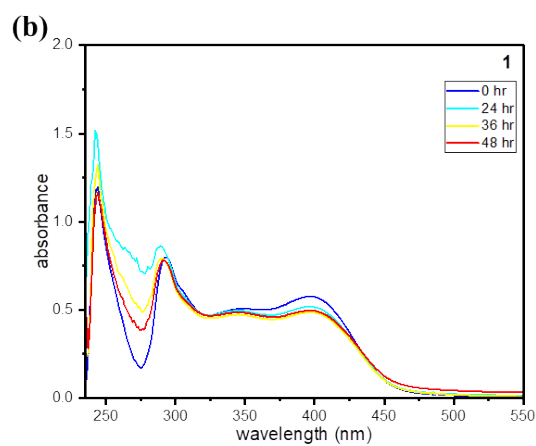
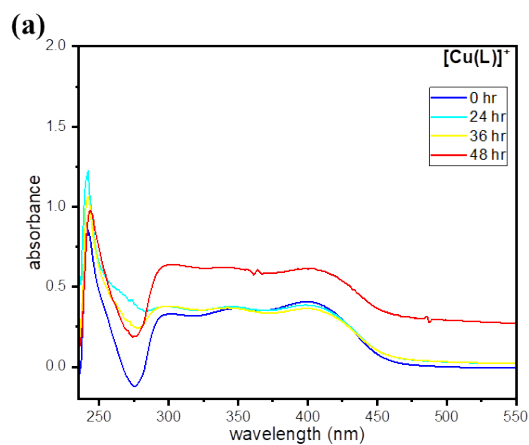
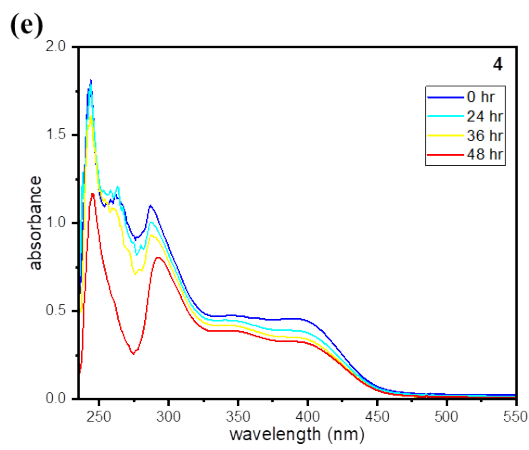
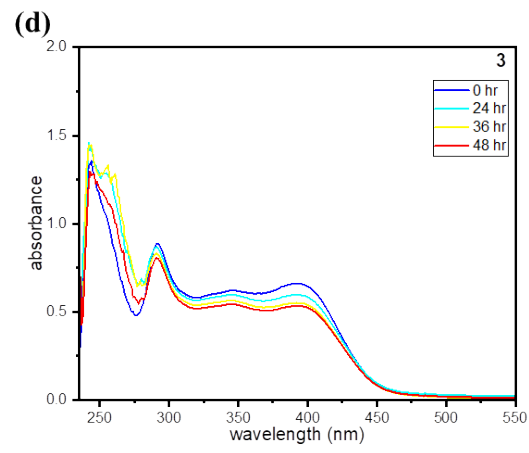
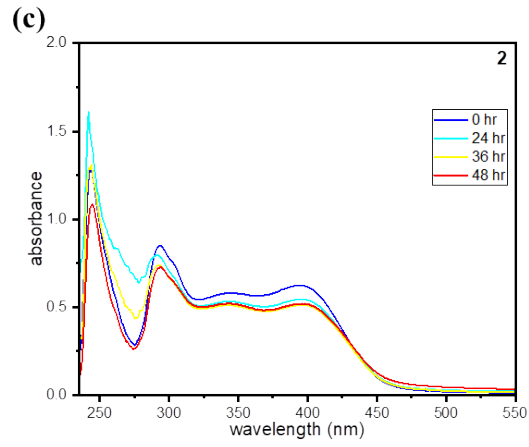


Figure S4. The stability of complexes in buffer was monitored using 0.5% DMSO-PBS pH 7.4 buffer at different time intervals 0, 24, 36, 48 h at 37 °C.





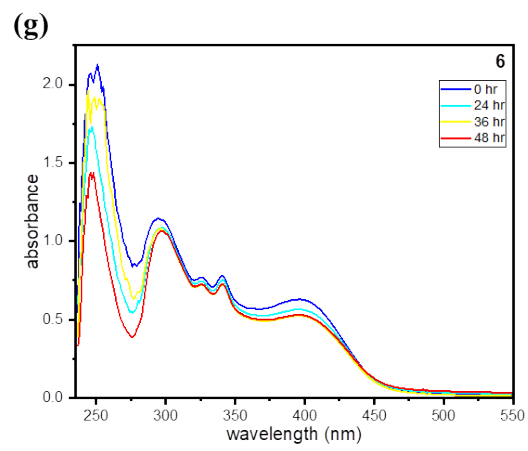
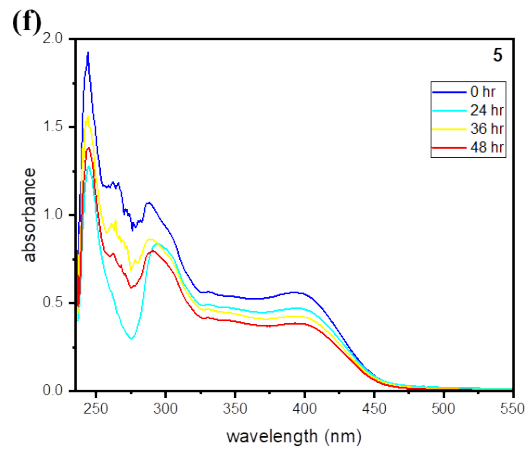


Figure S5. The stability of cell culture medium was monitored using 0.5% DMSO-RPMI (without phenol red) cell culture medium at different time intervals 0, 24, 36, 48 h at 37 °C.

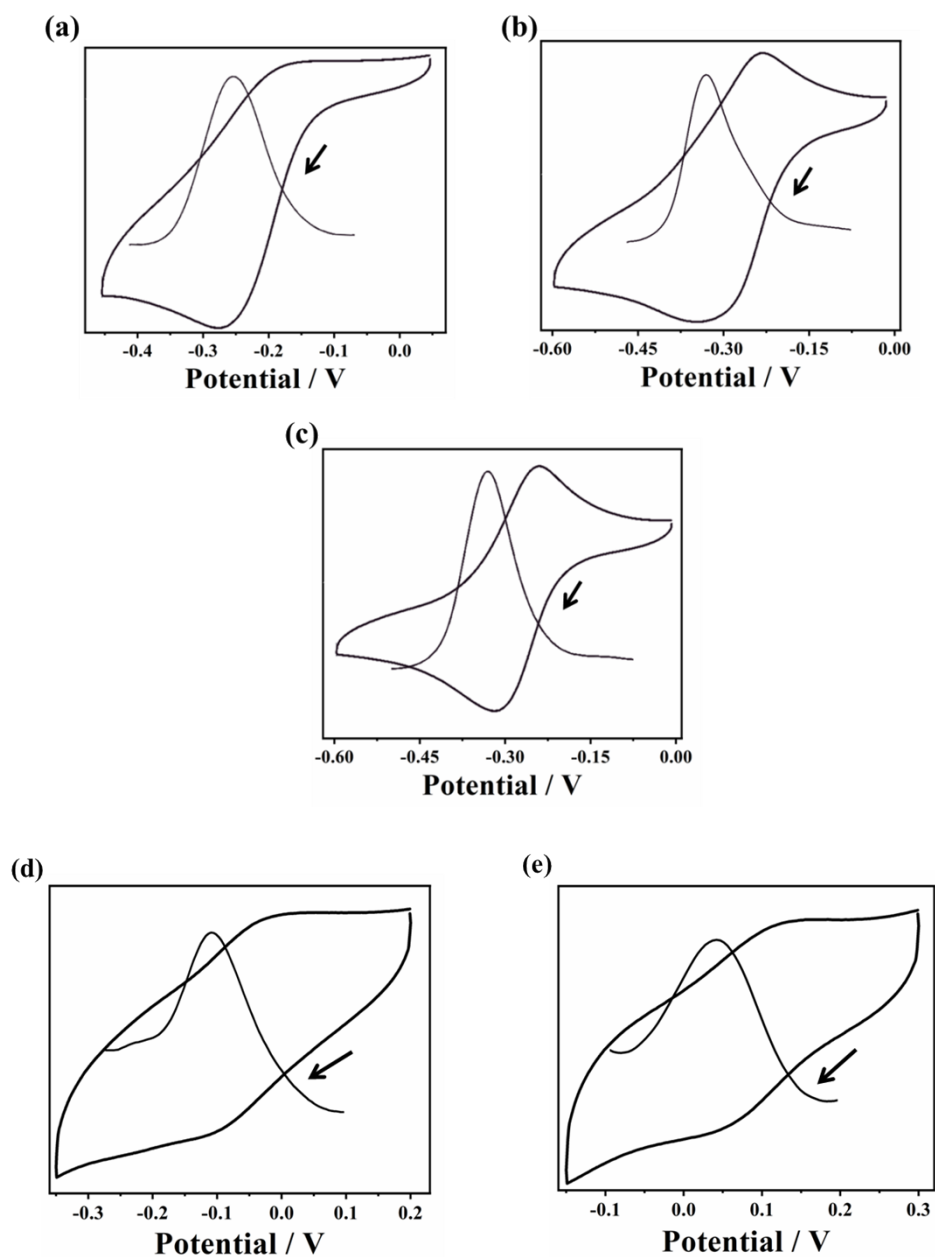


Figure S6. (a-e) Cyclic and differential pulse voltammograms of complexes $[\text{CuL}]^+$, **1**, **2**, **5**, and **6** in DMF respectively. Scan rate, $50 \text{ mV}\cdot\text{s}^{-1}$ and $5 \text{ mV}\cdot\text{s}^{-1}$; supporting electrolyte, Tetra-*N*-butylammonium perchlorate (0.1 M); Complex concentration, $1 \text{ mmol}\cdot\text{dm}^{-3}$.

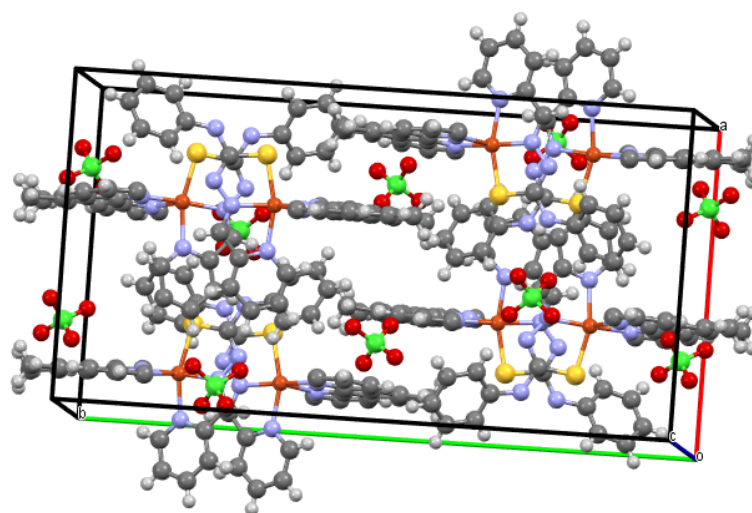


Figure S7. The packing diagram of $[\text{Cu}(\text{L})(5,6\text{-dmp})](\text{ClO}_4)_4$.

Table S2. Computed bond lengths of copper(II) complexes $[\text{CuL}]^+$ and **1-6**.

Bonds	Bond Lengths (Å)						
	$[\text{CuL}]^+$	1	2	3	4	5	6
Cu – N(1)	2.026	2.084	2.086	2.077	2.082	2.084	2.081
Cu – N(2)	1.996	2.007	2.008	2.008	2.008	2.008	2.006
Cu – S(1)	2.369	2.444	2.447	2.439	2.441	2.444	2.433
Cu – N(3)	-	2.195	2.187	2.232	2.215	2.213	2.232
Cu – N(4)	-	2.016	2.010	2.023	2.019	2.014	2.027
Cu – O(1)	1.997	-	-	-	-	-	-

Table S3. Computed bond angles [$^\circ$] of copper(II) complexes ($[\text{CuL}]^+$ and **1-6**).

Bond angles	$[\text{CuL}]^+$	1	2	3	4	5	6
N(1) – Cu(1) – N(2)	82.18	80.89	80.80	81.02	80.92	80.84	81.00
N(1) – Cu(1) – S(1)	166.11	155.92	155.58	157.12	156.64	156.17	157.82
N(1) – Cu(1) – N(4)	-	100.06	100.04	100.46	100.28	100.07	100.37
N(1) – Cu(1) – N(3)	-	99.36	98.89	98.59	98.41	98.48	97.15
N(2) – Cu(1) – S(1)	83.92	81.86	81.83	81.99	81.96	81.87	82.20
N(2) – Cu(1) – N(4)	-	171.67	172.25	171.43	171.97	171.64	171.34

N(2) – Cu(1) – N(3)	-	108.73	108.14	108.06	107.82	108.06	108.80
S(1) – Cu(1) – N(4)	-	94.69	94.95	94.19	94.56	94.74	94.16
S(1) – Cu(1) – N(3)	-	102.02	102.76	101.17	101.88	102.41	101.91
N(3) – Cu(1) – N(3)	-	79.36	79.42	80.15	79.95	80.09	79.60
N(1) – Cu(1) – O(1)	97.35	-	-	-	-	-	-
N(2) – Cu(1) – O(1)	179.51	-	-	-	-	-	-
S(1) – Cu(1) – O(1)	96.54	-	-	-	-	-	-
Trigonality index, τ	-	0.26	0.27	0.24	0.25	0.25	0.22

Table S4. Computed HOMO and LUMO energies and energy gap of copper(II) complexes $[\text{CuL}]^+$ and 1-6.

Complex Energy (eV)							
	$[\text{CuL}]^+$	1	2	3	4	5	6
Optimized energy	-2.731×10^4	-3.871×10^4	-4.084×10^4	-4.078×10^4	-4.292×10^4	-4.506×10^4	-4.583×10^4
HOMO	-6.3345	-6.1329	-6.1343	-6.1617	-6.1146	-6.1354	-6.1773
LUMO	-3.2047	-2.9407	-2.9195	-2.9416	-2.9318	-2.9133	-2.9579
Energy Gab	3.1299	3.1922	3.2148	3.2202	3.1828	3.222	3.2194

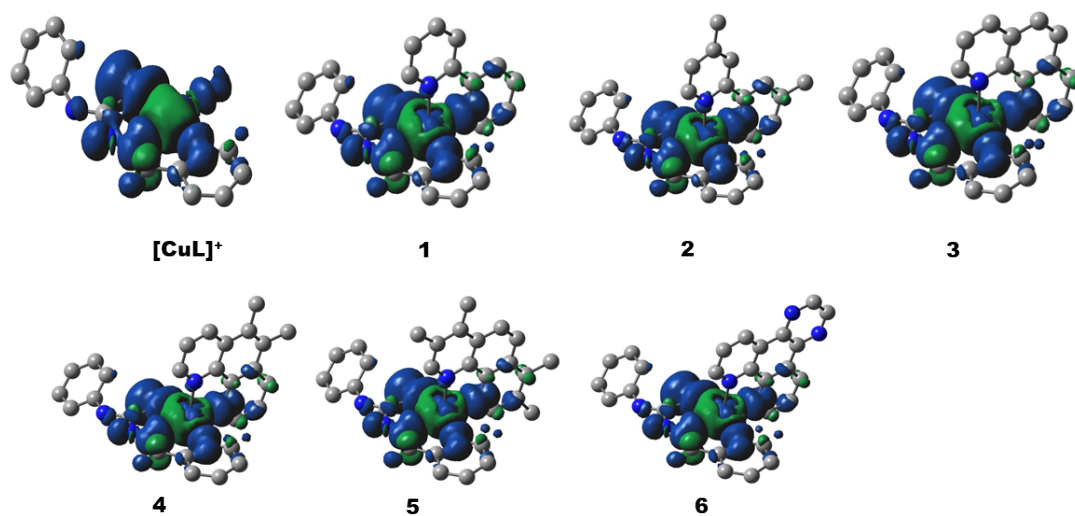


Figure S8. Spin Density plot of copper(II) complexes $[\text{CuL}]^+$ and 1-6.

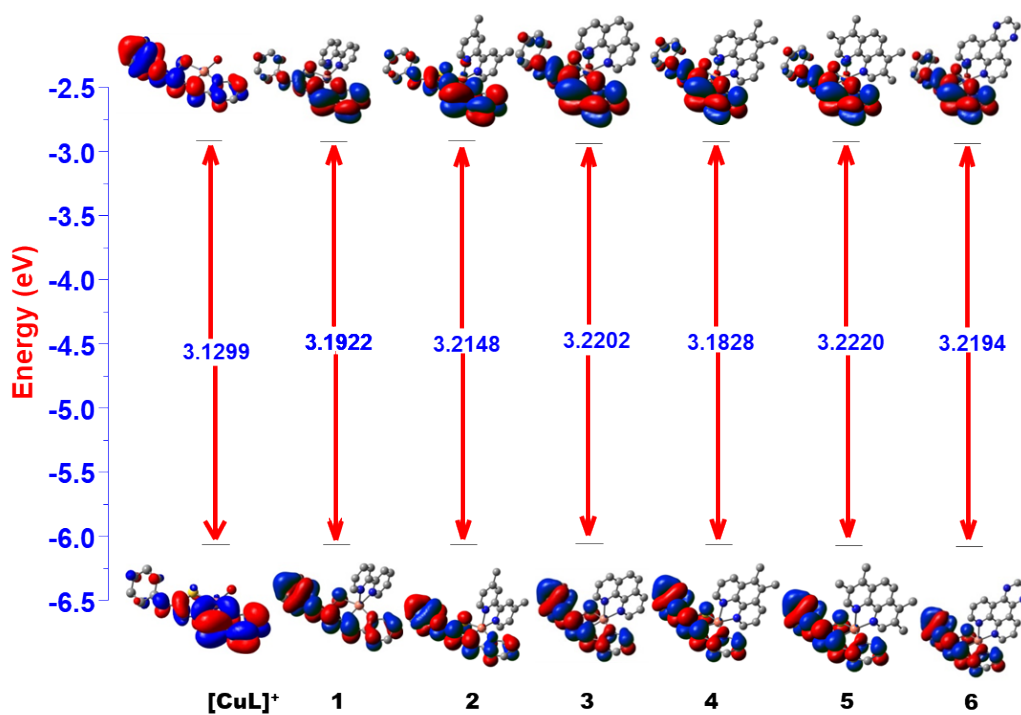


Figure S9. HOMO and LUMO band gap Energy profile diagram for complexes $[\text{CuL}]^+$ and 1-6 were calculated in B3LYP level of theory with mixed basis set LANL2DZ/6-31G and ACN as a solvent in CPCM method.

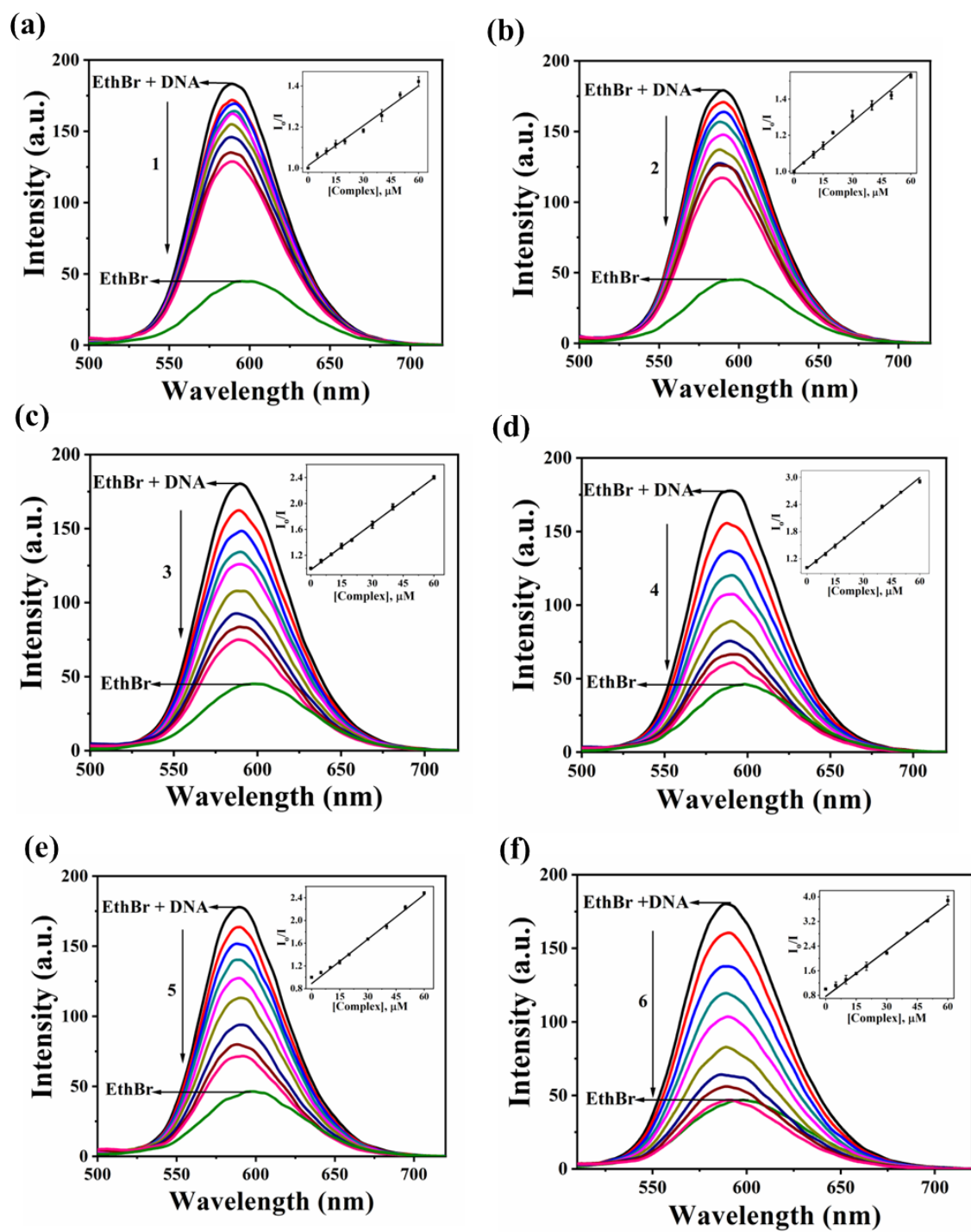


Figure S10. (a)-(f) Fluorescence titration of the copper(II) complexes 1-6 (0-60 μM) with DNA (125 μM). Inset: plot of I_0/I vs. [DNA] and the best fit curve.

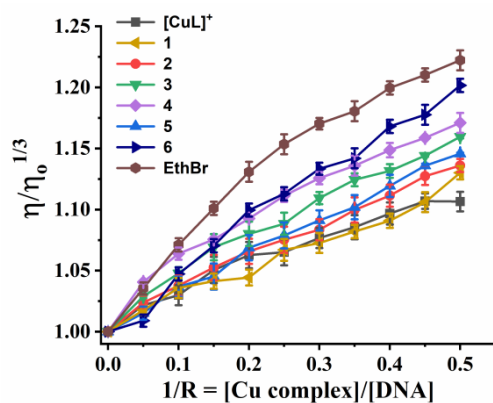


Figure S11. The effect of addition of complexes $[\text{CuL}]^+$ and 1-6 on the viscosity of CT DNA in 10% DMF-Tris-HCl buffer; Relative specific viscosity vs. $1/R$; $[\text{DNA}] = 500 \mu\text{M}$.

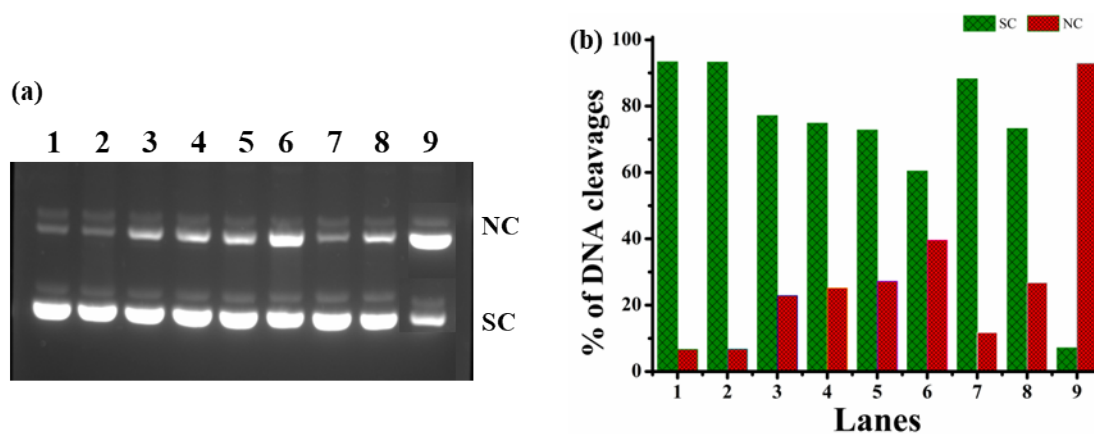


Figure S12. (a) Gel electropherogram showing the self-activated cleavage of supercoiled pUC19 DNA ($40 \mu\text{M}$ in base pair) by complexes $[\text{CuL}]^+$ and 1-6 ($100 \mu\text{M}$) at 4 h incubation: 1) pUC19 DNA; 2) pUC19 DNA + $[\text{CuL}]^+$; 3) pUC19 DNA + 1; 4) pUC19 DNA + 2; 5) pUC19 DNA + 3; 6) pUC19 DNA + 4; 7) pUC19 DNA + 5; 8) pUC19 DNA + 6; 9) pUC19 DNA + $\text{Cu}(\text{dpq})_2(\text{H}_2\text{O})]^{2+}$. (b) A graph shows the percentage of SC and NC forms of DNA exist in each lane with an incubation time of 4 h.

Table S5. Cleavage data of SC pUC19 DNA by copper(II) complexes $[\text{CuL}]^+$ and **1-6** in the absence of an activator for an incubation time of 4 h.

S.No.	Reaction conditions	% of cleavage	
		SC	NC
1	DNA	93	7
2	DNA + $[\text{CuL}]^+$	93	7
3	DNA + 1	77	23
4	DNA + 2	75	25
5	DNA + 3	73	27
6	DNA + 4	60	40
7	DNA + 5	88	12
8	DNA + 6	73	27
9	DNA + $[\text{Cu}(\text{dpq})_2]^{2+}$	7	93

Table S6. Cleavage data of SC pUC19 DNA by copper(II) complexes $[\text{CuL}]^+$ and **1-6** (100 μM) in the presence of reductant ascorbic acid (50 μM) for an incubation time of 1 h.

S.No.	Reaction conditions	% of cleavage	
		SC	NC
1	DNA	89	11
2	DNA + H ₂ A	73	27
3	DNA + H ₂ A + $[\text{CuL}]^+$	81	19
4	DNA + H ₂ A + 1	86	14
5	DNA + H ₂ A + 2	84	16
6	DNA + H ₂ A + 3	0	100
7	DNA + H ₂ A + 4	0	100
8	DNA + H ₂ A + 5	31	69
9	DNA + H ₂ A + 6	5	95
10	DNA + H ₂ A + $[\text{Cu}(\text{dpq})_2]^{2+}$	0	100

Table S7. Cleavage data of SC pUC19 DNA by copper(II) complexes phen (**3**) and 5,6-dmp (**4**) (50 μM) in the presence of reductant ascorbic acid (25 μM) for an incubation time of 1 h.

S.No.	Reaction conditions	% of cleavage	
		SC	NC
1	DNA	96	4
2	DNA + H ₂ A	94	6
3	DNA + H ₂ A + 3	18	82
4	DNA + H ₂ A + 4	11	89

Table S8. Cleavage data of SC pUC19 DNA by complex 5,6-dmp (**4**) in the presence of reductant ascorbic acid (50 μ M) and various ROS scavengers at 1 h incubation time.

S.No.	Reaction conditions	% of cleavage	
		SC	NC
1	DNA	89	11
2	DNA + H ₂ A	73	27
3	DNA + H ₂ A + 4 + DMSO	81	19
4	DNA + H ₂ A + 4 + NaN ₃	86	14
5	DNA + H ₂ A + 4 + Catalase	84	16
6	DNA + H ₂ A + 4 + SOD	0	100
7	DNA + H ₂ A + 4 + N ₂	0	100

Table S9. Cleavage data of SC pUC19 DNA by copper(II) complexes [CuL]⁺ and **1-6** (50 μ M) in the presence of reductant ascorbic acid (25 μ M) for an incubation time of 1 h under hypoxic conditions.

S.No.	Reaction conditions	% of cleavage	
		SC	NC
1	DNA	90	10
2	DNA + H ₂ A	81	19
3	DNA + H ₂ A + [CuL] ⁺	83	17
4	DNA + H ₂ A + 1	85	15
5	DNA + H ₂ A + 2	85	15
6	DNA + H ₂ A + 3	32	68
7	DNA + H ₂ A + 4	0	100
8	DNA + H ₂ A + 5	63	37
9	DNA + H ₂ A + 6	76	24

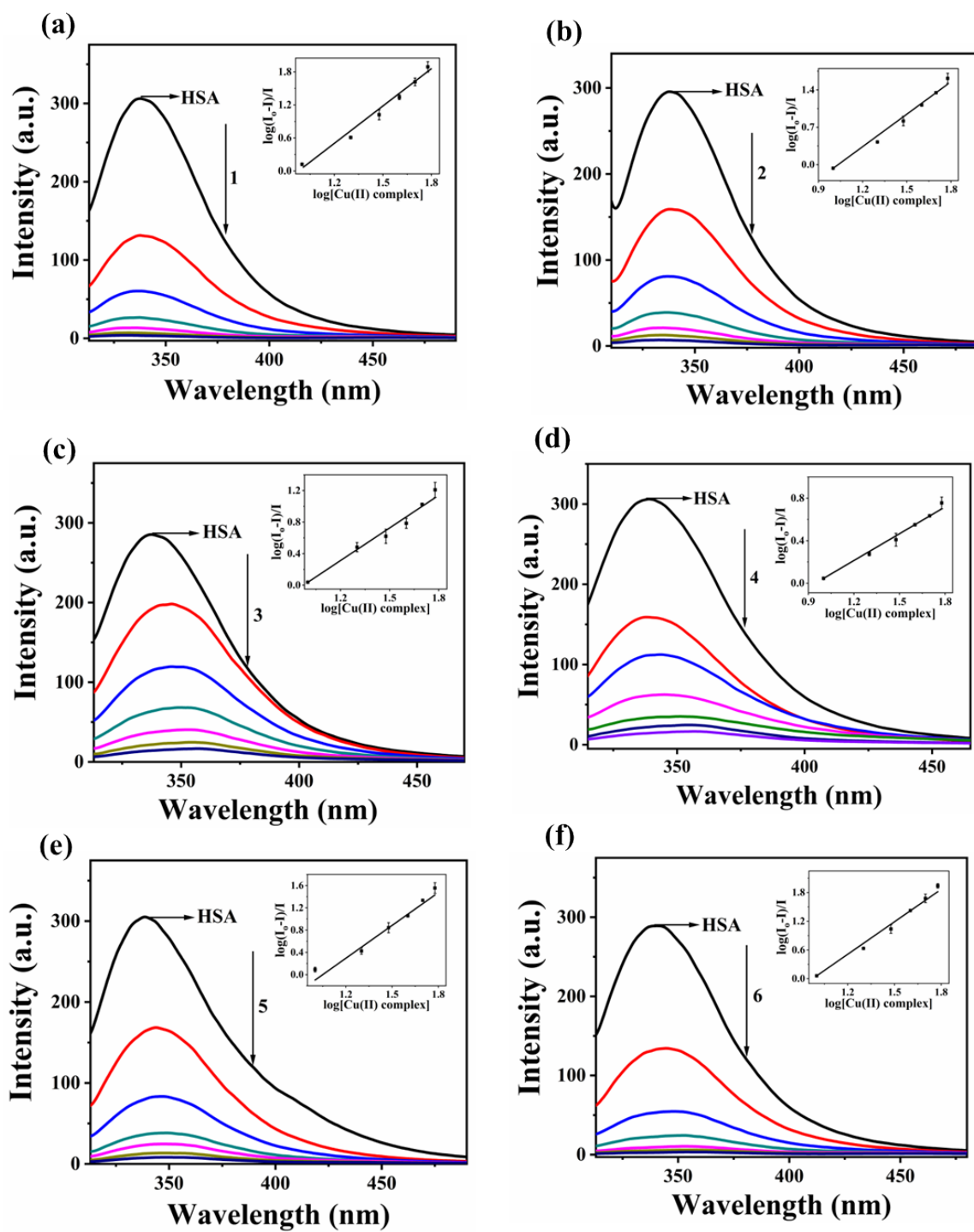


Figure S13. (a)-(f) The fluorescence of HSA was gradually quenched upon increasing the concentration of copper(II) complexes 1-6 at around 347 nm at pH 7.1. Inset: Scatchard plot of 1-6 was plotted at pH 7.1.

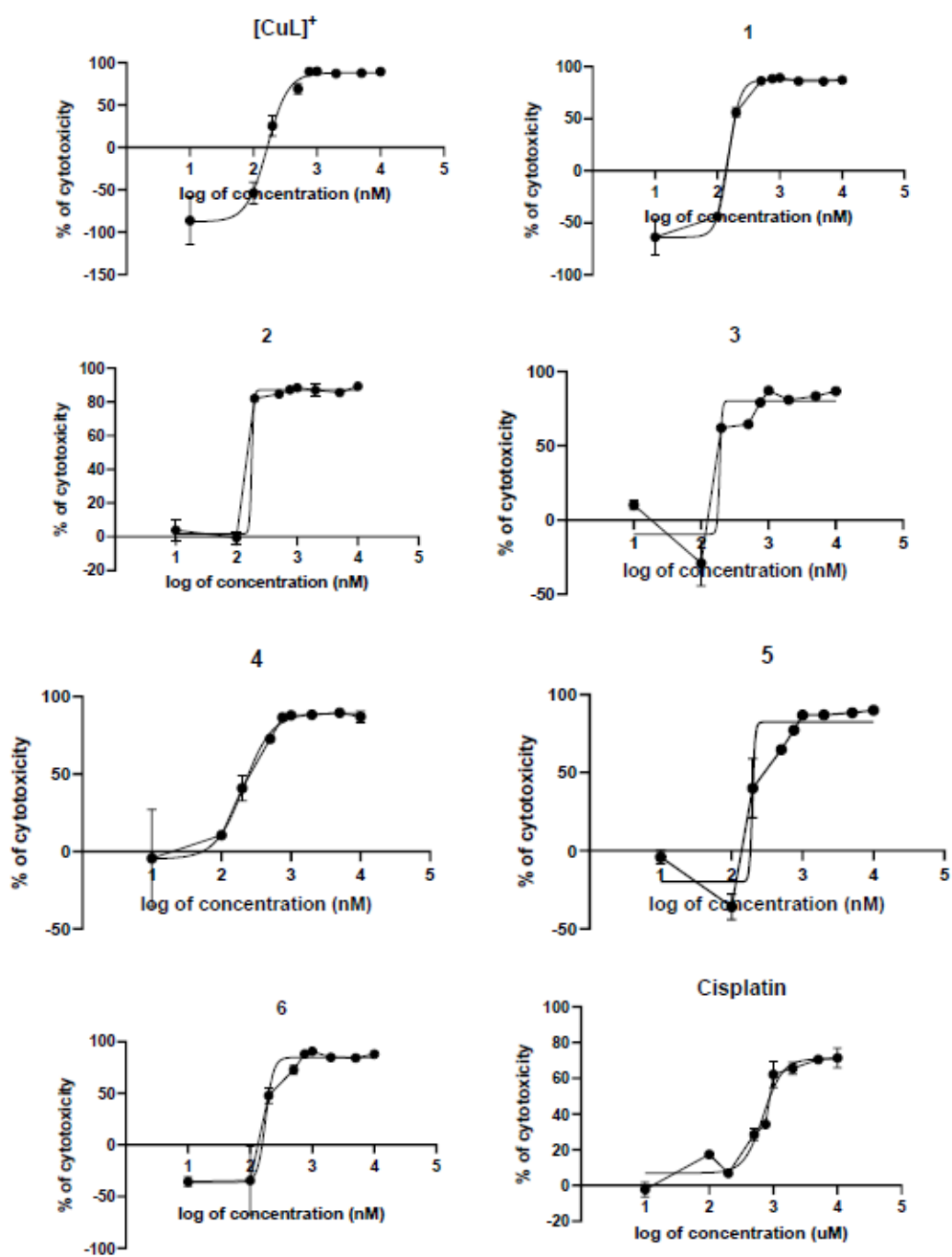


Figure S14. (a)-(h) Graph representing percentage cytotoxicity of compounds [CuL]⁺, 1-6 and cisplatin on HeLa cells at 24 h.

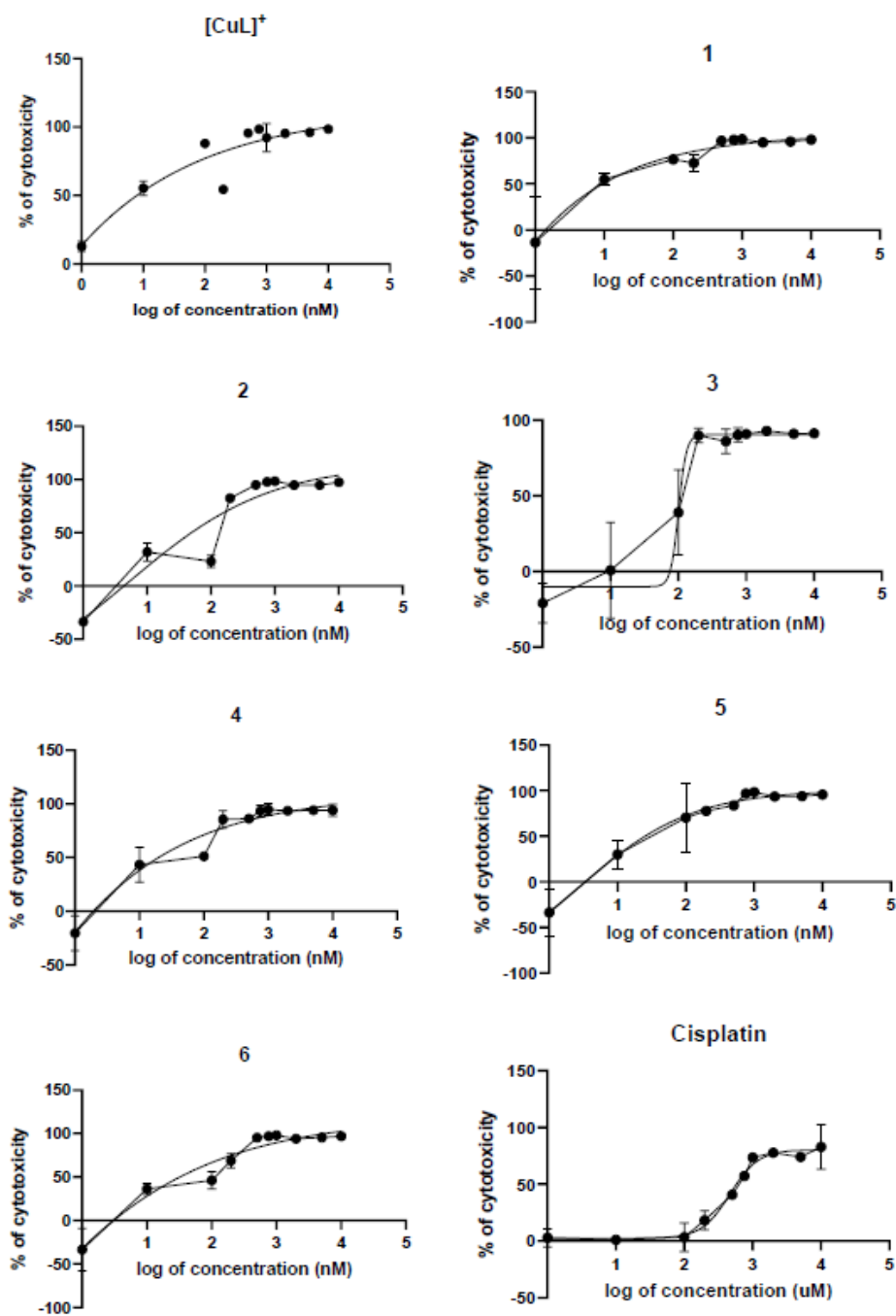


Figure S15. (a)-(h) Graph representing percentage cytotoxicity of compounds [CuL]⁺, 1-6 and cisplatin on HeLa cells at 48 h.

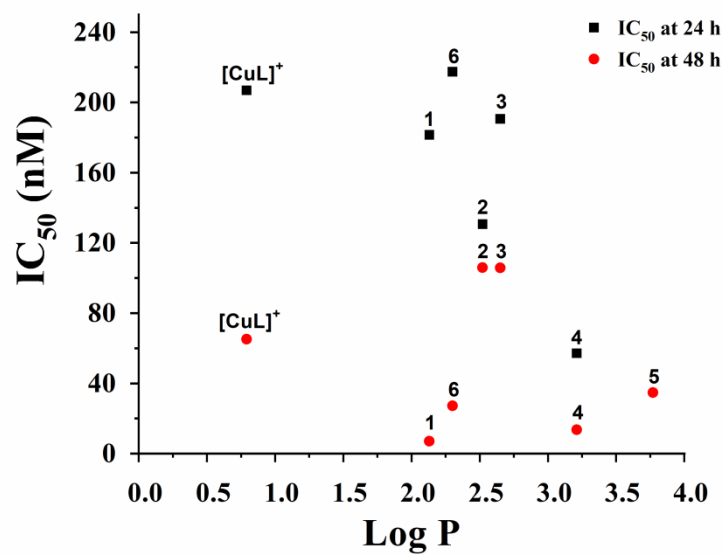


Figure S16. Relationship between the lipophilicity (Log P) and IC₅₀ values.

References

- 1 V. Rajendiran, R. Karthik, M. Palaniandavar, H. Stoeckli-Evans, V. S. Periasamy, M. A. Akbarsha, B. S. Srinag and H. Krishnamurthy, *Inorg. Chem.*, 2007, **46**, 8208–8221.
- 2 G. Cohen and H. Eisenberg, *Biopolymers*, 1969, **8**, 45–55.
- 3 X. Zou, B. Ye, H. Li, J. Liu, Y. Xiong and L. Ji, *Journal of the Chemical Society, Dalton Transactions*, 1999, **441**, 1423–1428.
- 4 J. K. Barton, J. M. Goldberg, C. V Kumar and N. J. Turro, *Journal of the American Chemical Society*, 1986, **108**, 2081–2088.
- 5 J. Bernadou, G. Pratviel, F. Bennis, M. Girardet and B. Meunier, *Biochemistry*, 1989, **28**, 7268–7275.
- 6 N. P. Singh, M. T. McCoy, R. R. Tice and E. L. Schneider, *Experimental Cell Research*, 1988, **175**, 184–191.
- 7 N. S. Quiming, B. Vergel, G. Nicolas and J. A. Villanueva, *J. Health Sci.*, 2005, **51**, 8–15.
- 8 Y. Q. Wang, H. M. Zhang, G. C. Zhang, W. H. Tao and S. H. Tang, *Journal of Luminescence*, 2007, **126**, 211–218.